2015 International Symposium on Nonlinear Theory and its Applications
NOLTA2015, Kowloon, Hong Kong, China, December 1-4, 2015

Noise Modelling of Fractional Capacitor and Noise Performance Analysis of Fractional Order Filter

M. Tripathy† and M. Khanra‡ and K. Biswas∗ and S. Sen∗

†Dept. of Electrical Engineering, CET, Bhubaneswar, Odisha, India
‡Dept. of Electronics & Instrumentation Engg., NIT Silchar, Assam–788010, India
∗ Dept. of Electrical Engineering, IIT Kharagpur, Kharagpur–721302, WB, India
Email: madhab.tripathy@gmail.com, munmunkhanra@gmail.com, karabi@ee.iitkgp.ernet.in, ssen@ee.iitkgp.ernet.in

Abstract—This paper proposes an approach for modelling noise due to fractional capacitor (FC) realized using domino ladder network. The proposed noise model has been applied in analyzing noise in fractional order (FO) Sallen-Key filter. The output noise power spectral density of the FO filter has been calculated. The theoretical analysis and simulation studies show that the noise contribution due to FCs changes with the change in the order of FCs. However, the change may not be significant in comparison with the overall noise level of the circuit.

1. Introduction

In analog circuit design, noise is a disturbance that interferes with the signal of interest. Noise also refers to any undesired excitations which exhibit random behavior [1], [2], [3] and is inherent to any analog circuit, arising from different sources. Due to such inherent noise levels of the constituent components, the analog circuits are limited to perceive small changes in input signals [4], [5].

Fractional order (FO) filter design and its realization are among the most recent areas of interest. FO filter circuits have been discussed thoroughly in literature [6], [7], however, noise analysis of these circuits is still in its early stage.

To study the noise performance of an electronic circuit, all the noisy components are replaced by their equivalent noise models [1]. The noise model of a resistor is a standard one and that of an OPAMP can be found in the corresponding data sheet [8]. Capacitors are considered to be ideal, not contributing the noise. However, the noise contribution due to FC [9], [10] and its effect on the noise level of the overall circuit is not known. This calls for the noise model of FC. In this work, the noise model of a FC is proposed by approximating it with a domino ladder (DL) circuit. The proposed noise model for FC has also been used to study the noise performance of FO filter.

Organization of the paper is as follows. A noise model for FC is proposed in Section 2. Using the proposed noise model, noise analysis of FO filters are performed in Section 3. The paper is concluded in Section 4.

2. Noise model of fractional capacitor

Ideally, all FCs, unlike conventional capacitors, are noisy in nature due to the existence of real impedance in the impedance expression of FCs. Analog realization of FC is approximately done using truncated RC network [11], [12]. In this work, FC realized using domino ladder (DL) circuit in Fig. 1 has been used for noise modelling and analysis.

The resistors and capacitors used in DL circuits form a

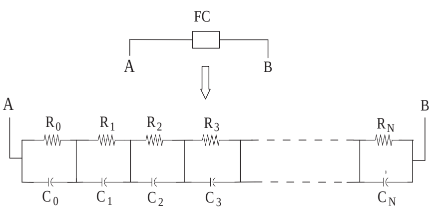

Figure 1: Domino ladder network for implementing FC

geometric progression as [11]:

$$R_j = g^{-j} R_0; \quad C_j = G^{-j} C_0; \quad (j = 1, \ldots, n) \quad (1)$$

The impedance of the DL network [11]:

$$Z(s) = 1/C_F s^{\alpha} \quad (2)$$

where, $\alpha = (1 - \nu)$, $\nu = \frac{ln(G)}{ln(Gg)}$, $\frac{1}{C_F} = \frac{\pi cosec(\pi\nu) R_0^{\nu}}{ln(Gg) C_0^{1-\nu}}$ and $0 < \nu < 1$. The order α of the FC can be varied by assigning different values of g and G [11]. Similarly, the bandwidth of FC can be varied by varying the product $R_0 C_0$ [12].

Thermal noise is modeled by a noise voltage e having spectral density S in series with a noiseless resistor R. Noise voltage e and PSD S can be expressed as

$$e = \sqrt{4 k_b T R \Delta f} \ (V) \quad (3)$$

$$S^2 = 4 k_b T R \ \left(V^2/Hz\right) \quad (4)$$

where, 'k_b' is the Boltzmann's constant, 'T' is the absolute temperature in Kelvin and Δf is the noise equivalent bandwidth (ENBW) [1]. Therefore, the noise model of FC using DL circuit of Fig. 1 can be obtained by adding a thermal noise source to each resistor as shown in Fig. 2.

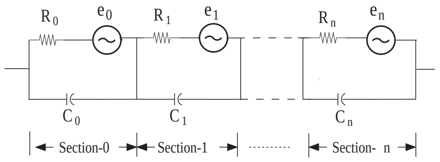

Figure 2: Noise model of FC realized using DL circuit

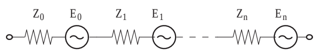

(a) Equivalent model of circuit in Fig. 2

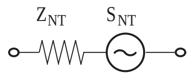

(b) Equivalent noise model of FC

Figure 3: Equivalent circuit models

Thermal noise of FC, using DL circuit, increases due to the presence of chain resistors. Power spectral density S_i corresponding to each noise source e_i can thus be expressed as $S_i = \frac{e_i^2}{\Delta f} = 4k_bTR_0 \frac{V^2}{Hz}$ [1]. Applying Thevenin equivalent to each section of the domino ladder circuit (Fig. 2), the equivalent noise model becomes a series combination of noise sources and their noise impedances as shown in Fig. 3(a) where, $E_i = \frac{Z_{C_i}}{R_i+Z_{C_i}}e_i$, $Z_i = R_i||Z_{C_i}$, Z_{C_i} is the impedance of C_i and $(i = 0,\ ...,\ n)$.

Mean square noise voltage of the FC:

$$\overline{V_{NT}^2} = \overline{(E_0 + \ .... \ + E_n)^2} = \overline{E_0^2} + \ ... \ + \overline{E_n^2} \qquad (5)$$

$$\overline{V_{NT}^2} = \frac{\overline{e_0^2}}{(1+R_0C_0s)^2} + \ .... \ + \frac{\overline{e_n^2}}{(1+R_nC_ns)^2} \qquad (6)$$

From Eqns. (1), (3) and (6), V_{NT}^2 can be expressed as

$$\left|\overline{V_{NT}^2}\right| = 4k_bT\Delta f \sum_{i=0}^{n} \frac{g^{-i}R_0}{1+g^{-2i}G^{-2i}R_0^2C_0^2\omega^2} \qquad (7)$$

The power spectral density (PSD) of the total noise (using the relation $\frac{ln(G)}{ln(Gg)} = 1-\alpha$ given after Eqn. (2))

$$S_{NT} = \left|\overline{V_{NT}^2}\right|/\Delta f = 4k_bTR_0 \sum_{i=0}^{n} \frac{g^{-i}}{1+G^{\frac{2i}{\alpha-1}}p^2\omega^2} \qquad (8)$$

and Z_{NT}, the total noise impedance:

$$Z_{NT} = Z_0 + Z_1 + ... + Z_n = 1/C_Fs^{\alpha} \qquad (9)$$

The overall noise model of FC is simplified to a noise PSD, S_{NT} in series with an impedance Z_{NT} shown in Fig. 3(b).

2.1. Effect of order α on output noise PSD

From Eqn. (8), it is clear that, the noise power spectral density of a FC depends on the frequency of operation ω, the parameter $p\,(= R_0C_0)$ and the order α. The variations of PSD are shown in Fig. 4.

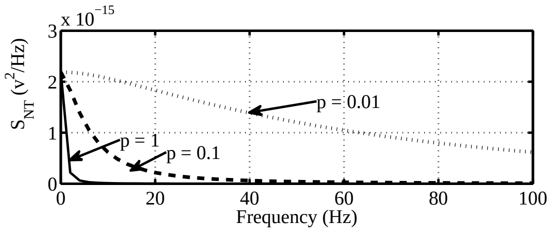

(a) $\alpha = 0.5$

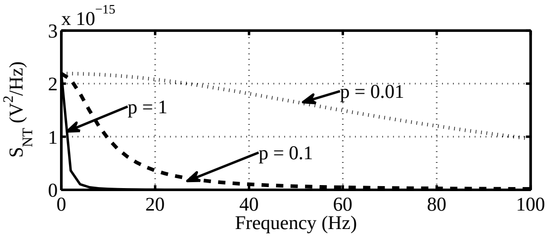

(b) $\alpha = 0.8$

Figure 4: Noise power spectral density of fractional capacitor for different α

Table 1: Components of DL circuits in calculating noise PSD due to FC ($n+1$: RC-sections in DL circuit)

R_0	C_F	$p\,(= R_0C_0)$	(n)
100 kΩ	$10^{-6}\ [F/s^{(1-\alpha)}]$	0.01, 0.1, 1	15

Here, the fractional capacitance (C_F) is kept constant with $C_F = 10^{-6}\ [F/s^{(1-\alpha)}]$. Component values chosen for simulation of noise PSD of FC are presented in Table 1.

2.2. Effect of component values chosen for domino ladder circuit on output noise PSD

Representation of FC using RC network is not unique. Even, with a fixed value of fractional capacitance (C_F) and order (α), the realization using DL network can be different with different values of R_0 and C_0, initially chosen. As a result, the noise model deployed in this section is not unique, that can be seen from Fig. 4(a) and 4(b). For a particular value of FC C_F, order (α), and $p\,(= R_0C_0)$, the value of G and g (as defined in Eqn. (1)) are fixed as shown in Table 2.

Table 2: Geometric ratios G and g used in DL network for FC, $C_F = 10^{-6}\ [F/s^{(1-\alpha)}]$

Order (α)	Geometric ratio 'G'			Geometric ratio 'g'		
	$p = 0.01$	0.1	1	$p = 0.01$	0.1	1
0.5	4.8	1.64	1.17	4.8	1.64	1.17
0.8	53.6	1.97	1.11	2.70	1.18	1.02

3. Noise analysis of fractional order Sallen-Key filter

The proposed noise model has been applied for analysis of noise in FO Sallen-Key filter shown in Fig. 5. The filter

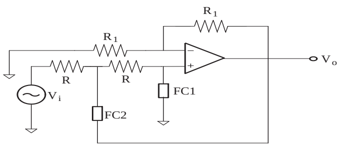

Figure 5: FO Sallen-Key filter using two FCs

contains two FCs: FC1 of order α and FC2 of order β ($0 < \alpha,\ \beta < 1$). For noise analysis, all the noisy components have been replaced by their equivalent noise models and the input signal sources have been shorted to ground. The noise model circuit is shown in Fig. 6 where, $e_1 = e_2$ and $e_{11} = e_{12}$ are the thermal noise voltages of R_1 and R respectively; Z_{NT1} and Z_{NT2} are the impedance; and V_{NT1} and V_{NT2} are the thermal noise voltages of FC1 and FC2 respectively. The transfer function of the filter:

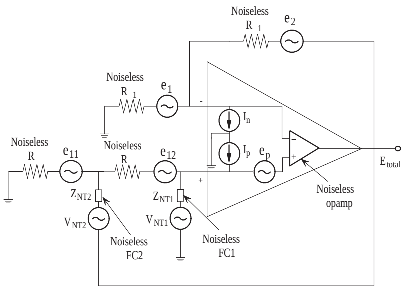

Figure 6: FO filter circuit incorporating noise sources.

$$H(s) = \frac{V_0(s)}{V_i(s)} = \frac{Ka^2}{s^{\alpha+\beta} + 2as^{\alpha} - as^{\beta} + a^2} \tag{10}$$

where, $K = 2$ is gain of the filter and $a = \frac{1}{RC_F}$.
Effect of individual noise source on the output PSD (Fig. 6) is calculated considering one noise source at a time while all other components are assumed to be noiseless. Finally, all the effects are added to evaluate the total noise effect. A noiseless OPAMP has been assumed to be ideal.

The filter parameter values used for simulation are presented in Table 3 where OPAMP specifications (I_n, I_p and e_p) are as per the data sheet [2].

3.1. Output noise PSD due to resistors

1) Output noise PSD due to resistors R_1 with noise source e_1 and e_2 are same and can be expressed as

$$\frac{\left|\overline{V_{0e1}}\right|^2}{\Delta f} = \frac{\left|\overline{V_{0e2}}\right|^2}{\Delta f} = 4k_bTR_1\frac{m+n+u}{m+n-u} \tag{11}$$

where, $m = \omega^{2(\alpha+\beta)} + a^2\omega^{2\beta} + 4a^2\omega^{2\alpha} + a^4$,
$n = 2a\omega^{(\alpha+2\beta)}\cos(\frac{\alpha\pi}{2}) + 4a\omega^{(2\alpha+\beta)}\cos(\frac{\beta\pi}{2}) + 4a^2\omega^{(\alpha+\beta)}\cos(\frac{(\alpha-\beta)\pi}{2})$, and $u = 2a^2(\omega^{(\alpha+\beta)}\cos(\frac{(\alpha+\beta)\pi}{2}) + a\omega^{\beta}\cos(\frac{\beta\pi}{2}) + 2a\omega^{\alpha}\cos(\frac{\alpha\pi}{2}))$.

Table 3: Component values used for simulation

Component	Value
R_1	1 kΩ
R	10 kΩ
C_F (both FC1, FC2)	$10^{-6}\ [F/s^{(1-\alpha)}]$
$a\ (= \frac{1}{RC_F})$	100
$\alpha,\ \beta$	0.5, 0.8, 1
$p\ (= R_0C_0)$	0.1, 0.1, 1
OPAMP	LF411
f_{nc}	50 Hz
I_n	$0.04 \times 10^{-12}\ \frac{A}{\sqrt{Hz}}$
I_p	$0.04 \times 10^{-12}\ \frac{A}{\sqrt{Hz}}$
e_p	$25 \times 10^{-9}\ \frac{V}{\sqrt{Hz}}$

2) Output noise PSD due to R with noise source e_{11}:

$$S_{e11} = \frac{\left|\overline{V_{0e11}}\right|^2}{\Delta f} = 4k_bTR\frac{4a^4}{m+q+r} \tag{12}$$

where, $q = 4a\omega^{(2\alpha+\beta)}\cos(\frac{\beta\pi}{2}) - 2a\omega^{(\alpha+2\beta)}\cos(\frac{\alpha\pi}{2}) - 4a^2\omega^{(\alpha+\beta)}\cos(\frac{(\alpha-\beta)\pi}{2})$ and $r = 2a^2(\omega^{(\alpha+\beta)}\cos(\frac{(\alpha+\beta)\pi}{2}) + 2a\omega^{\alpha}\cos(\frac{\alpha\pi}{2}) - a\omega^{\beta}\cos(\frac{\beta\pi}{2}))$.
3) Output noise PSD due to R with noise source e_{12}:

$$S_{e12} = 4k_bTR\frac{a^4 + a^2\omega^{2\beta} + 2a^3\omega^{\beta}\cos(\frac{\beta\pi}{2})}{m+q+r} \tag{13}$$

4) The total contribution in output noise PSD due to resistors can thus be calculated using Eqn. (14) and the corresponding response is shown in Fig. 7(a)

$$S_R = \frac{\left|\overline{V_{0e1}}\right|^2}{\Delta f} + \frac{\left|\overline{V_{0e2}}\right|^2}{\Delta f} + \frac{\left|\overline{V_{0e11}}\right|^2}{\Delta f} + \frac{\left|\overline{V_{0e12}}\right|^2}{\Delta f} \tag{14}$$

Output noise PSD due to resistors is more when $\alpha < \beta$ and its value decreases when $\alpha > \beta$ as 3-dB bandwidth of FO filter for $\alpha < \beta$ is more than that for $\alpha > \beta$ [7] and noise bandwidth is linearly proportional to 3-dB bandwidth. Values of equivalent noise bandwidth for different combinations of orders of FCs are given in Table 4.

3.2. Output noise PSD due to OPAMP

The output noise PSD due to OPAMP depends on e_p, I_p and I_n where, I_n and I_p are the noise current at inverting and non-inverting input respectively; and e_p is the input noise voltage. The input noise of an OPAMP contains thermal noise, shot noise and flicker noise [2]. Therefore, noise PSD due to OPAMP, S_{OP}, can be evaluated as a combinations of $\frac{1}{f}$ noise and white noise as:

$$E_{rms}(OP) = \sqrt{\int_0^{\Delta f} S_{OP}df + f_{nc}\int_0^{\Delta f}\frac{S_{OP}}{f}df} \tag{15}$$

where f_{nc} is the noise corner frequency [2].

Output noise PSD due to e_p, I_p, and I_n can individually be derived in similar manner. The contribution of noisy OPAMP on the output noise PSD is presented in Fig. 7(b).

3.3. Output noise PSD due to FCs

Output noise PSD due to FC1:

$$S_{FC1} = \frac{\left|\overline{V_{0VNT1}}\right|^2}{\Delta f} = \left|\overline{S_{NT1}}\right| \\ \frac{K^2(\omega^{2(\alpha+\beta)}+4a^2\omega^{2\alpha}+4a\omega^{(2\alpha+\beta)}\cos(\frac{(\alpha+\beta)\pi}{2}))}{m+q+r} \quad (16)$$

Output noise PSD due to FC2 can be obtained similarly; and the total output noise PSD due to FCs is $S_{FC} = S_{FC1} + S_{FC2}$. The response is shown in Fig. 7(c).

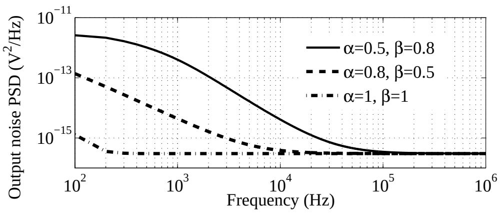

(a) PSD due to resistors

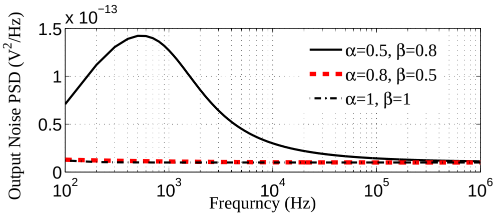

(b) PSD due to OPAMP

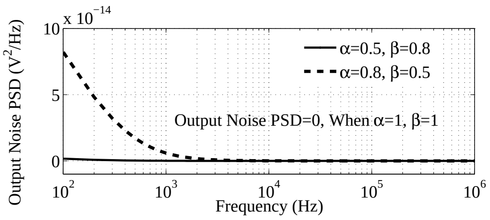

(c) PSD due to fractional capacitors (F_{C1} and F_{C2})

Figure 7: Output Noise PSD of FO Sallen-Key filter

3.4. Total output noise of the FO Sallen-Key filter

Total output noise of FO filter can be calculated combining the noise contributions due to resistors, fractional capacitors and OPAMP; and given in Table 4.

4. Conclusion

A noise modeling technique for FC is proposed. Using this approach, the noise analysis of FO Sallen-Key filter circuit has been carried out. It is observed that the noise contribution of FCs on over all noise level of the circuit varies with the orders of FCs. To the best of the authors' knowledge, the approach used in this paper is being reported for the first time. Further studies on noise analysis based on more fundamental concepts are needed to develop a systematic approach on noise analysis of fractional order circuits. Moreover, the noise analysis, in this work, has been done based on approximate model, DL network. Therefore, further developments should be based on both actual model and fabricated device. Work is going on the detailed study and experimental validation.

Table 4: Total noise voltage (E_{rms}) of the FO filter (Δf: equivalent noise bandwidth, E_{rms}: total noise voltage)

(α, β)	(0.5, 0.8)	(0.8, 0.5)	(1, 1)
f_{3dB} (Hz)	120.3	11.56	15.91
Δf (Hz)	2.91×10^2	37	25
E_{rms} (volt)	3.62×10^{-6}	1.42×10^{-6}	2.04×10^{-6}

References

[1] R. Pallas-Areny and J. G. Webster, *Analog Signal Processing*. John Wiley and Sons, New York, 1999.

[2] T. Instruments, *Noise analysis on operational Amplifier circuits*. Application report, 2007.

[3] H. Weinrichter and J. A. Nossek, "Noise analysis of active-RC filters," in *Proceedings of International Symposium on Circuits and Systems (ISCAS)*, April 1976, pp. 344–347.

[4] L. T. Bruton, F. N. Trofimenkoff, and D. H. Treleaven, "Noise performance of low-sensitivity active filters," *IEEE Journal of Solid-State Circuits*, vol. 8, pp. 85–91, 1973.

[5] A. S. Sedra and P. Brackett, *Filter Theory and Design*. Pitman, London, 1978.

[6] B. Maundy, A. S. Elwakil, and T. J. Freeborn, "On the practical realization of higher order filters with a fractional stepping," *Signal Processing*, vol. 91, pp. 484–491, 2011.

[7] M. C. Tripathy, K. Biswas, and S. Sen, "A design example of a fractional order Kerwin-Huelsman-Newcomb (KHN) biquad filter with two fractional capacitors of different order," *Circuits, Systems and signal processing*, vol. 32(4), pp. 1523–1536, August, 2013.

[8] "LF411 low offset, low drift JFET input operational amplifier," http://www.ti.com/lit/ds/symlink/lf411-n.pdf, accessed on 20 February 2013.

[9] K. Biswas, S. Sen, and P. K. Dutta, "Realization of a constant phase element and its performance study in a differentiator circuit," *IEEE Transactions on Circuits and Systems - II*, vol. 53, pp. 802–806, 2006.

[10] M. S. Krishna, S. Das, K. Biswas, and B. Goswami, "Fabrication of a fractional order capacitor with desired specifications: A study on process identification and characterization," *IEEE Transactions on Electron Devices*, vol. 58, no. 11, pp. 4067–4073, 2011.

[11] K. B. Oldham and C. G. Zoski, "Analogue instrumentation for processing polarographic data," *Journal of Electroanalytical Chemistry*, vol. 157, pp. 27–51, 1983.

[12] D. Mondal and K. Biswas, "Performance study of fractional order integrator using single-component fractional order element," *IET Circuits, Devices and Systems*, vol. 5, no. 4, pp. 334–342, 2011.